JBC Papers in Press. Published on July 9, 2012 as Manuscript M112.349852
The latest version is at http://www.jbc.org/cgi/doi/10.1074/jbc.M112.349852



# Ligand mimicking receptor variant discloses binding and activation mode of prolactin releasing peptide*

**Daniel Rathmann[1,4], Diana Lindner[1,3,4], Stephanie H. DeLuca[2,4], Kristian W. Kaufmann[2], Jens Meiler[2] and Annette G. Beck-Sickinger[1,*]**

[1]From the Institute of Biochemistry, Faculty of Biosciences, Pharmacy and Psychology, Universität Leipzig, Brüderstrasse 34, 04103 Leipzig, Germany; [2] Vanderbilt University Center for Structural Biology, 5144B Biosci/MRBIII, 465 21st Avenue South, Nashville, TN 37232-8725, USA

*Running title: *CAM of PrRP receptor reveals binding & activation site*

To whom correspondence may be addressed: Annette G. Beck-Sickinger, Institute of Biochemistry, Universität Leipzig, Brüderstrasse 34, 04103 Leipzig, Germany. Tel.: (0049) 341-9736901; Fax: (0049) 341-9736909; E-mail: beck-sickinger@uni-leipzig.de

**Keywords:** constitutively active mutants; GPCR; ligand docking; PrRP receptor; Rosetta modeling

**Background:** Constitutively active mutants (CAM) of G-protein coupled receptors are often related to human diseases.
**Results:** Novel type of CAM mimicking the ligand revealed a double binding mode of the PrRP/receptor and its binding pocket.
**Conclusions:** Modeling guided mutagenic approach discloses distinct insights into the molecular mechanisms ligand recognition and activation.
**Significance:** Concept can be adopted to study hereditary harmful CAM and assist GPCR-based drug development.

## ABSTRACT

**The prolactin-releasing peptide receptor (PrRPR) and its bioactive RF-amide peptide (PrRP20) have been investigated to explore the ligand binding mode of peptide G-protein coupled receptors (GPCR). By receptor mutagenesis we identified the conserved aspartate in the upper part of transmembrane helix 6 ($D^{6.59}$) of the receptor as the first position that directly interacts with arginine 19 of the ligand ($R^{19}$). Permutation of $D^{6.59}$ with $R^{19}$ of PrRP20 led to $D^{6.59}R$, which turned out to be a constitutively active receptor mutant (CAM). This suggests that the mutated residue at the top of transmembrane helix 6 mimics $R^{19}$ by interacting with additional binding partners in the receptor. Next, we set up a comparative model of this CAM because no ligand docking is required, and selected a next set of receptor mutants to find the engaged partners of the binding pocket. In an iterative process we identified two acidic residues and two hydrophobic residues that form the peptide ligand binding pocket. As all residues are localized on top or in the upper part of the transmembrane domains we clearly can show that the extracellular surface of the receptor is sufficient for full signal transduction for PrRP, rather than a deep membrane binding pocket. This contributes to the knowledge of the binding of peptide ligands to GPCR and might facilitate the development of GPCR ligands, but also provides new targeting of CAM involved in hereditary diseases.**

## INTRODUCTION

Identification of direct receptor-ligand interactions for the approximately 800 identified G protein-coupled receptors (GPCR) is as challenging as it is important for drug discovery (1) as 50% of all currently available drugs target the specific manipulation of GPCR activity (2-3). The PrRP receptor superfamily is expressed in almost all cells/tissues, is involved in a plethora of different signalling pathways, and plays an important role in a large variety of physiological processes.

The prolactin-releasing peptide receptor (PrRPR) was originally isolated from rat hypothalamus (4). PrRPR has been detected widely throughout the human and rat brain (5) and most commonly activates the $G_q$ protein-coupled signalling pathway (6). Its eponymous endogenous ligand, the prolactin-releasing peptide (PrRP), was identified in 1998 by a reverse pharmacology approach on the basis of orphan GPCR (7-8).

PrRP features two equipotent isoforms, PrRP31 (31 residues) and an N-terminally truncated PrRP20 (20 residues) (6,8). PrRP is an RF-amide peptide, consisting of a common carboxy-terminal arginine (R) and an amidated phenylalanine (F) motif and plays a role in energy metabolism, stress responses, circadian rhythm, analgesia, and in anorexigenic effects (7,9). Structure-activity relationship studies of PrRP using N-terminally truncated mutants and alanine substitution within these constructs (10-12) demonstrated the biological significance of the C-terminal R and F residues, and the amidation of the C-terminus.

Site-directed mutagenesis is a powerful and widely used tool to study receptor activation. This approach alone can provide insight in the function of GPCR, but it is often used in combination with information provided by other techniques, such as crystallography or molecular modeling, in order to relate receptor function to a tertiary structure (13). The conserved $D^{6.59}$ residue of the Y receptor (YR) family was shown to interact with a specific R of either human pancreatic polypeptide or neuropeptide Y (NPY) in a subtype-specific manner (14-15). The numbering of receptor residues has been performed as suggested by Ballesteros and Weinstein (16). PrRPR shares its phylogenic origin with Y receptors (17), leading to sequence similarities (Figure 1A) and a number of conserved residues, including $D^{6.59}$ (Figure 1C). Furthermore, the ligands of these receptors are structurally similar (18) and share a similar C-terminal sequence (Figure 1B). While the RF-amide motif was previously identified as a major requirement for PrRP-induced agonist activity (10-11), the critical residues on the receptor remain unknown, and the ligand binding mode is still poorly understood.

Here, we describe the first mutagenesis study of the human PrRP receptor (PrRPR). We used the extracellular region to elucidate the binding site and the molecular mechanism of GPCR activation. Considering the relevance of the C-terminal R and F residues of PrRP for receptor binding, we applied the concept of double cycle mutagenesis approach (15,19-20) and identified the first direct contact point between PrRP20 and the PrRPR, consisting of the conserved $D^{6.59}$ and the $R^{19}$ residue of PrRP20. To prove the existence of this interaction, we switched the residues involved in the salt bridge formation and created $D^{6.59}R$ PrRPR and $D^{19}$PrRP20. This newly introduced R in the receptor variant $D^{6.59}R$ might serve as surrogate for the absent $R^{19}$ of the ligand as it led to a new type of constitutive activity. Given the lack of data of experimentally determined structures of peptide GPCR, we developed a comparative model of the human PrRPR. By combining molecular modelling with double cycle mutagenesis experiments in the framework of this constitutively active mutant (CAM), we conceived an effective strategy to explore structural determinants of ligand recognition on a molecular level. More specifically, we were able to identify $Y^{5.38}$, $W^{5.28}$, $E^{5.26}$, and to some extend $F^{6.54}$ to be involved in receptor activation and ligand binding. This combinatory approach enabled us to clarify the double binding mode of $R^{19}$ of the peptide ligand, which has two putative interaction partners within the PrRPR, $E^{5.26}$ and $D^{6.59}$. The assembled experimental data were used to generate a model of the PrRP/receptor interaction in molecular detail. Furthermore our data describe the binding mode of a peptide ligand to GPCR by solely interacting with residues localized in the extracellular domain or upper part of the TM helices. In our approach we identified a receptor mutant with constitutive activity, which most likely relies on mimicking a direct ligand-receptor interaction. This provides knowledge on the function of an active mode of GPCR and may be applied to other peptide GPCR.

## EXPERIMENTAL PROCEDURES

*Peptide synthesis.* Rink amide resin (NovaBiochem; Läufelfingen, Switzerland) was used to synthesize PrRP20, $A^{19}$PrRP20, $D^{19}$PrRP20, and $A^{20}$PrRP20 by automated solid phase peptide synthesis (Syro; MultiSynTech, Bochum, Germany) as previously described, using the orthogonal Fmoc/$^t$Bu (9-fluorenyl-methoxycarbonyl-*tert*-butyl) strategy (21). Purification and verification of the peptides was achieved as previously described (Table S1) (22).

*DNA extraction from SMS-KAN.*To obtain genomic DNA from SMS-KAN cells (human neuroblastoma cells, DSMZ, Braunschweig, Germany), approximately 1 million cells were digested overnight at 55°C with 500 µl lysis buffer

(1 M NaCl, 20% SDS, 0.5 M EDTA, 1 M Tris, pH 8.5 was adjusted using hydrochloric acid (HCl)) containing 50 µg proteinase K (Promega, Mannheim, Germany). Genomic DNA was extracted using phenol/chloroform and precipitated from the aqueous phase with isopropanol, washed with ethanol and then dissolved in water.

*Cloning and mutagenesis of the PrRP receptors in eukaryotic expression vectors.* The coding sequence of the human PrRPR was obtained by PCR amplification from the isolated genomic DNA of SMS-KAN cells and cloned into the eukaryotic expression vector pEYFP-N1 (Clontech, Heidelberg, Germany) C-terminally fused to EYFP, using the *Xho*I and *Bam*HI restriction site to result in the construct phPrRPR_EYFP-N1. The correctness of the entire coding sequence was confirmed by DNA sequencing using the dideoxynucleotide (ddNTP) termination method developed by Sanger (23). Plasmids encoding single point mutations (Table I-II) were prepared by using the QuikChange™ site-directed mutagenesis method (Stratagene, CA, USA) with the desired mutagenic primers. For intermolecular double-cycle mutagenesis approaches, the single alanine mutated receptor constructs were investigated, using single alanine modified PrRP20 analogs. Plasmids encoding double mutations containing $Y^{2.64}A$, $W^{2.71}A$, $E^{5.26}A$, $E^{5.26}R$; $W^{5.28}A$, $D^{6.59}A$, $F^{6.54}A$ or $Q^{7.35}A$ as a second mutation, respectively, were prepared by using the QuikChange™ site-directed mutagenesis approach with the $D^{6.59}R$ or $D^{6.59}A$ construct as template. In addition, all PrPR receptor constructs were also generated N-terminally fused to the coding sequence of the hemagglutinin (HA)-tag. The entire coding sequence of each resulting receptor mutant was proven by sequencing.

*Cell culture.* Cell culture material was supplied by PAA Laboratories GmbH (Pasching, Austria). Culture of COS-7 (African green monkey, kidney), HEK293 (human embryonic kidney), and SMS-KAN cells was done as recommended by the supplier (DSMZ, Braunschweig, Germany). Briefly, cells were grown as monolayers at 37°C in a humidified atmosphere of 5% $CO_2$ and 95% air. COS-7 cells were cultured in Dulbecco's Modified Eagle's Medium containing 10% (v/v) heat-inactivated fetal calf serum (FCS), 100 units/ml penicillin and 100 µg/ml streptomycin and HEK293 cells were grown in DMEM / Ham' F12 (1:1) without L-glutamine containing 15% (v/v) heat-inactivated FCS as previously described (15,24). SMS-KAN cells were maintained in nutrient mixture Ham's F12 / Dulbecco's modified Eagle medium (1:1) with 15% (v/v) FCS, 4 mM glutamine, and 0.2 mM non-essential amino acids (25).

*Fluorescence microscopy.* HEK293 cells ($1.2x10^5$) were seeded into 8-well chamber slides (ibidi, Munich, Germany). The transient transfection of HEK293 cells were performed using 0.1 µg to 1µg vector DNA and 1 µl Lipofectamin™ 2000 transfection reagent (Invitrogen GmbH, Karlsruhe, Germany) according to the manufacturer's instructions. The nuclei were visualized with Hoechst 33342 (1 µg/ml; Sigma Aldrich, Taufkirchen, Germany) for 10 min after 1h of starving with OPTI®-MEM I Reduced Serum Medium (Invitrogen GmbH, Karlsruhe, Germany). Fluorescence images were obtained using an ApoTome Imaging System with an Axio Observer microscope (Zeiss, Jena, Germany). All investigated receptors were correctly integrated in the membrane as confirmed by live-cell microscopy (Figure S1A).

*Quantification of receptor cell surface localisation by cell surface ELISA.* To quantify plasma-membrane receptors, a cell surface ELISA was performed using an antibody directed against the native 15 N-terminal amino acids of the PrRPR. 50 000 HEK293 cells were grown in 96-well plates and transfected with the PrRP wt receptor or its mutants after reaching 75-85% of confluence. The cells were starved with OPTI®-MEM I (30 min) 17 hours post-transfection and fixed in 4% paraformaldehyde (30 min). For immune-staining, cells were blocked with 2% BSA and permeabilized with 0.5% Triton X-100, 2% BSA in Dulbecco's Modified Eagle's Medium for 1 hour (37°C) to determine total receptor amounts, whereas surface expressed receptors were quantified without permeabilization. Incubation was performed with the primary antibody (1:2000 dilutions) for 2 hours (25°C) and followed by 1.5 hour (25°C) incubation with the secondary antibody (1:5000). Receptors were

detected by using rabbit anti-N-terminus (GPR10 antibody [N1], GTX108137, GeneTex) followed by horseradish peroxidase-conjugated goat anti-rabbit IgG (sc-2004, Santa Cruz, Heidelberg, Germany). The results were fully confirmed in a second independent ELISA set up, using a peroxidise-conjugated anti-HA-antibody (1:1000 dilutions, 12CA5, Roche, Mannheim, Germany) versus the N-terminally fused HA-tag of the generated PrRPR constructs (data not shown). Quantification of the bound peroxidase was performed as described and analysis performed with the GraphPad Prism 5.03 program (14). Values are presented as mean values ± s.e.m. of four individual experiments, measured in triplicates.

*Radioligand binding studies.* For radioligand binding studies, $1.5 \times 10^6$ COS-7 cells were seeded into 25 $cm^2$ flasks. At 60-70% confluency, cells were transiently transfected using 4 µg vector DNA and 15 µl of Metafectene™ (Biontex Laboratories GmbH, Martinsried/Planegg, Germany). Approximately 24 h after transfection binding assays were performed on intact cells using N [propionyl-$^3$H] hPrRP20. Binding was determined with 1 nM N [propionyl-$^3$H] hPrRP20 in the absence (total binding) or in the presence (non-specific binding) of 1 µM unlabeled hPrRP20, respectively, as described previously (26-27). Our former evaluated protocol (28) was used to obtain N [propionyl-$^3$H] hPrRP20 by selective labelling with a specific activity of 3.52 TBq/mmol and resulting in a $K_d$-value of 0.58 nM. Specific binding of each PrRP receptor mutant was compared to specific binding of the PrRP wt receptor. $IC_{50}$-values and the $K_d$-value were calculated with GraphPad Prism 5.03 (GraphPad Software, San Diego, USA), fitted to a one-site competition or a one-site binding model, respectively. Triplicates were measured in at least two independent experiments for the determination of $IC_{50}$-values, whereas one experiment in triplicate was made for $K_d$-value estimation.

*Signal transduction assay.* Signal transduction (inositol phosphate, or IP, accumulation) assays were performed as previously described with minor modifications (22). The time of incubation was increased to 3 h for the double mutants of PrRPR and reduced to 1h for measurement of concentration-response curves. To test for constitutive activity, COS-7 cells were incubated without agonist for 1 h, 3 h, and 6 h at 37°C. Each ligand-receptor interaction was analyzed with the GraphPad Prism 5.03 program by establishing the corresponding data set from different experiments. All signal transduction assays were repeated at least twice independently and measured in duplicate. The global curve fitting function of GraphPad Prism 5.03 was asked to determine given $EC_{50}$-ratios. The statistical significance of relevant samples was computed by using the unpaired student's t-test, based on the means, values with $P < 0.05$ were considered to be significant.

*Multiple sequence alignment.* ClustalW (29) was used to align the primary sequence of the PrRPR with the sequences of mammalian Y and PrRP receptors. Next, the transmembrane regions of six GPCR of known structure (see below) were structurally aligned with Mustang (30). The profiles resulting from these first two steps were then aligned to one another with ClustalW, and the human PrRPR sequence alignment used for modelling was taken from this final profile-profile alignment. The C-terminal 310 residues of the PrRPR primary sequence were threaded onto the 3D coordinates of six available GPCR experimental structures; PDBIDs: 1U19 (31), 3CAP (32), 3DQB (33), 2RH1 (34), 2VT4 (35), 3EML (36).

*Construction of the comparative models.* Extracellular loop regions were reconstructed using kinematic loop closure (37) and cyclic coordinate descent (CCD) (38) as implemented in the ROSETTA v3 software suite. The models were refined with the ROSETTA v3 all-atom energy function. Energetically favourable models were grouped into 15 structurally similar groups by k-means clustering, and the lowest scoring models of each cluster were analysed. Models based on the template PDB 3DQB had the lowest energy and were used to inform the mutagenesis studies.

*Model refinement and peptide docking.* The comparative model constructed in light of the new mutagenesis data was generated using the original multiple sequence alignment. To model

the PrRPR/ligand complex, an iterative peptide docking and loop remodeling procedure was performed: Energetically favorable changes in orientation were determined using the ROSETTAMEMBRANE all-atom energy function (39)**.** The PrRP8-20 model was docked into the putative binding site of the receptor while allowing remodeling of ELs 1, 2, and 3. Using the ROSETTADOCK protocol (40)**,** translational movements of the peptide of up to 4Å were allowed in three dimensions and the peptide was allowed to rotate along its x, y, and z-axes by up to 10°. Loop regions were constructed using cyclic coordinate descent (CCD) (38). The conformational search was enhanced by conducting the modeling in the presence of loose distance restraints where models that placed $D^{6.59}$, $E^{5.26}$, $W^{5.28}$, and $Y^{5.38}$ within 10Å of $R^{19}$ of the peptide were more energetically favorable than those that did not. The PrRP8-20 model was generated by *de novo* folding the peptide using ROSETTANMR with sparse NMR chemical shift and distance data (41). Of 19,241 PrRP/receptor complex docked models, the top ten by total score were analyzed. Two of these models were considered structurally redundant, leaving eight unique models that agree with the experimental data presented herein (Figure 8).

## RESULTS

*$R^{19}$ of the endogenous ligand PrRP20 interacts with the $D^{6.59}$ of PrRPR.* Based on the data of the NPY/YR system (14-15), we hypothesized $D^{6.59}$ to be the interaction partner of $R^{19}$ in the PrRP/PrRPR system. To test this hypothesis, charge and size prerequisites in position $D^{6.59}$ were elucidated by systematic substitution to $D^{6.59}$A, $D^{6.59}$E, $D^{6.59}$N, $D^{6.59}$R, and $D^{6.59}$K (Table 1). The expected impact on function was confirmed by the right-shifted concentration-response curve of $D^{6.59}$A, compared to the wildtype (wt) receptor after stimulation with PrRP20 (Figure 1D). The increased $EC_{50}$-value (26 nM) of the $D^{6.59}$A mutant confirms the importance of the $D^{6.59}$ side chain. In addition, the results obtained for the other $D^{6.59}$ single mutants support the hypothesis of an ionic interaction; $D^{6.59}$E behaves similarly to wt, the oppositely charged $D^{6.59}$K shows strong effects in potency and the bulkier, more positively charged $D^{6.59}$R is not tolerated (Table 1). The impact of the substitutions increases as follows: E<A<K<R, showing that the lack of charge is a first critical component. This is followed by necessities in space and strength of the opposing charged K and R at position 6.59, suggesting different and increasing repulsion of the substitutions by PrRP20 stimulation (Table 1). Therefore, the charge seems to be a major prerequisite at position 6.59.

The signal transduction results obtained for PrRPR stimulation with peptide analogs $A^{19}$PrRP20 and $A^{20}$PrRP20 confirmed the essential influence of the formerly described RF-amide motif with respect to binding and signaling (Table 1, S1 & S2) (10-12). Circular dichrosim (CD) spectroscopy showed that these variations have no influence on the PrRP20 overall structure, at least, not detectable by CD (data not shown).

*Double cycle mutagenesis suggests additional receptor region "X" critical for peptide binding.* The concentration-response curve of the $D^{6.59}$A receptor with PrRP20 reveals a 15-fold elevated $EC_{50}$-value (Figure 2A; Table 1), whereas the wt receptor stimulated with $A^{19}$PrRP20 results in a 736-fold elevated $EC_{50}$-value (Figure 2B; Table 1). This finding suggests that $R^{19}$ has one or more additional interaction partner, "X," which explains the increased importance of $R^{19}$for receptor activity. Stimulation of the $D^{6.59}$A receptor with $A^{19}$PrRP20 resulted in a 0.16-fold elevated $EC_{50}$-value, compared to PrRP20 stimulation. This non-additive effect of the double cycle mutagenesis experiment implies that the effects of the individual replacements are not independent of each other. Among more complicated mechanisms, such as indirect interactions of the two residues, the effect may also be due to a direct interaction between $D^{6.59}$ of PrRPR and $R^{19}$ of PrRP20 (Figure 2C; Table 1).

*Reciprocal mutagenesis leads to a constitutively active receptor mutant.* To confirm the direct interaction between $R^{19}$ and $D^{6.59}$, the corresponding residues were swapped (Figure 3A). The herein performed reciprocal mutagenesis approach assumes that a lost interaction between two residues induced by single mutation to the counter amino acid can partly be recovered by a second mutation that establishes the interaction in

a reverse manner. We used this method to verify the salt bridge between $D^{6.59}$ and $R^{19}$ in the PrRP/PrRPR system by using the single peptide $D^{19}$PrRP20 and the $D^{6.59}$R receptor mutant (Figure 3C). The single peptide mutant $D^{19}$PrRP20 shows a similar effect as $A^{19}$PrRP20, with an increased $EC_{50}$-value of 1318 nM (Table 1) without impact on the efficacy (Figure 3B). We conclude that all peptide-receptor interactions that involve position $R^{19}$ have been disrupted (Figure 2B, 3B). In the reverse experiment, PrRP20 barely stimulated the $D^{6.59}$R receptor mutant with no determinable $EC_{50}$-value (Figure 3C). In comparison to both single mutant experiments, the activation of the $D^{6.59}$R but also $D^{6.59}$K mutant with $D^{19}$PrRP20 revealed a gain of function ($EC_{50}$-values: $D^{6.59}$R = 138 nM and $D^{6.59}$K = 115 nM, Table 1; Figure 3C & 4C), confirming the direct interaction of $R^{19}$ and $D^{6.59}$. At the same time, the experiment provides further evidence in support of a second interaction site "X" for $D^{6.59}$R, as the $EC_{50}$-value is still elevated by a factor of 84 compared to the wt interaction.

A novel possibility to identify the missing interaction site "X" arose because the $D^{6.59}$R receptor mutant presented a strongly increased basal activity, which is indicated by curves with higher initial IP accumulation (Figure 3C &4C). In contrast, $D^{6.59}$A and $D^{6.59}$K reveal solely slight elevated basal activity. This can be explained by more loosened constraints at this position and thus making it more susceptible for induced basal activity, whereas for $D^{6.59}$K the spatial and more charged prerequisites are missing. The observed effect of constitutive activity is independent of transient transfection, which is a critical component. Different amounts of transfected DNA resulted in essentially similar cellular responses (Figure 4A). Finally, the constitutive activity of the $D^{6.59}$R receptor mutant was confirmed by an increased time-dependent IP-accumulation compared to wt (Figure 4B; 1h, 3h = $P < 0.05$; 6h = $P < 0.01$). All investigated receptors were correctly integrated in the membrane as confirmed by live-cell microscopy (Figure S1A) and revealed similar cell surface levels as determined by surface ELISA (Figure S1B & S1C).

*Identification of "X" by modelling-guided double mutant analysis.* We hypothesize that $D^{6.59}$R PrRPR is a CAM caused by the interaction of $D^{6.59}$R with residue "X." $D^{6.59}$R mimics $R^{19}$ of PrRP20, inducing a partially active receptor conformation (Figure 4D). We further hypothesize that $D^{6.59}R/X^{X.X}A$ double mutants will lose constitutive activity and most importantly, retain activation by $D^{19}$PrRP20. In order to determine likely positions for "X," a comparative model of the PrRPR was constructed using the ROSETTA molecular modelling software suite. Details of the modelling protocol are given in the Materials and Methods. According to the lowest-energy model based on the semi-active opsin structure (PDBID: 3DQB (32)). $E^{5.26}$, $W^{5.28}$, $Y^{5.38}$, $F^{6.54}$, and $Q^{7.35}$ were found proximal to $D^{6.59}$ and were proposed to be potential interaction partners for $D^{6.59}$R (Figure 5A) or for $R^{19}$PrRP20 when testing the wt receptor. The more distant residues, $Y^{2.64}$ and $W^{2.71}$, were chosen for control experiments.

With guidance from the receptor modelling data (Figure 5A), we generated and tested the double mutants $Y^{2.64}A/D^{6.59}R$, $W^{2.71}A/D^{6.59}R$, $E^{5.26}A/D^{6.59}R$, $W^{5.28}A/D^{6.59}R$ $Y^{5.38}A/D^{6.59}R$, $F^{6.54}A/D^{6.59}R$, and $Q^{7.35}A/D^{6.59}R$ of PrRPR. Interestingly, $E^{5.26}A/D^{6.59}R$, $W^{5.28}A/D^{6.59}R$, and $Y^{5.38}A/D^{6.59}R$ receptor mutants completely lost their constitutive activity in a ligand-independent signal transduction assay (Figure 5B). The IP accumulation after three hours of these unstimulated receptors dropped to a PrRPR wt level. The $F^{6.54}A/D^{6.59}R$ dropped as well but remained partially constitutively active (Figure 5B). These effects could be due to disruption of the hypothesized interaction to the $R^{6.59}$ residue or to decisive structural alterations, resulting in generally non-functional mutants. The latter situation was excluded after activation of these constructs using 10 µM $D^{19}$PrRP20 as an agonist (Figure 5B; $P<0.01$). In concentration-response experiments the $EC_{50}$-values were determined to be higher than 100 µM (Figure 6A). The fact that $D^{19}$PrRP20, not wt PrRP20, was able to activate these constructs re-emphasizes the direct interaction of $D^{19}$ with $D^{6.59}$R.

Other double mutants, such as $Y^{2.64}A/D^{6.59}R$ or $Q^{7.35}A/D^{6.59}R$, showed slightly reduced constitutive activity but seem to be trapped in that state, as no further activation/stimulation was achieved. $W^{2.71}A/D^{6.59}R$ appears to have structural restrictions because no significant receptor activation could be observed. From the plethora of residues in the upper TMHs and ELs of PrRPR, which may interact with $D^{6.59}$R

the initial comparative models and mutational studies clearly suggested seven residues to potentially interact with $D^{6.59}$R. Of these seven potential interaction sites, we hypothesize $E^{5.26}$, $W^{5.28}$, $Y^{5.38}$, and $F^{6.54}$ to be engaged in $D^{6.59}$R-induced basal activity. Therefore, we postulate the latter residues to be involved in ligand binding and/or receptor activation. The combination of mutagenesis and comparative modelling enabled us to extract three residues of relevance from the plethora of residues in the upper transmembrane helices (TMHs) and extracellular loops (ELs) of the PrRPR.

*Confirmation of binding and activation site using single mutants.* To clarify the exact impact of the identified positions $E^{5.26}$, $W^{5.28}$, $Y^{5.38}$, and $F^{6.54}$, single alanine mutants at these positions were generated. Signal transduction studies of the single alanine mutants $E^{5.26}$A (331-fold over wt), $W^{5.28}$A (580-fold over wt), $Y^{5.38}$A (61-fold over wt), and $F^{6.54}$A (15-fold over wt) confirm the impact of residues $E^{5.26}$, $W^{5.28}$, $Y^{5.38}$, and $F^{6.54}$ on ligand binding (Table 2, Figure 6B). Their distribution in EL2 and TMH5 suggests that this region plays a significant role in ligand binding. Therefore, EL2 and TMH5 were studied systematically to identify additional interaction sites that might have been missed due to inaccuracies of the comparative model. All charged (R, K, E, D) and aromatic (W, F, Y) residues between positions 4.65 and 5.40 were substituted to alanine (Table 2). None of the tested mutants resulted in significantly increased $EC_{50}$-values (Figure 6B, Table 2). This demonstrates that the model-guided intramolecular mutagenesis experiment, at least in this setting, was more effective than alanine scanning in selecting the critical interaction partners.

To verify the obtained results of potency of the PrRP wt receptor and its mutants, the cellular expression levels in the plasma membrane were investigated, because recently a constitutive internalization of the PrRP receptor has been reported (42). Binding studies of transiently transfected COS-7 cells revealed a sufficient number of surface wt receptors per cell (~95 000), calculated from the obtained $B_{max}$-value (445 Bq), the specific activity ($3.52*10^{15}$ Bq/mol) and cell number ($6.6*10^{5}$). All PrRP receptor constructs with impact on potency were shown to be surface exposed and quantified by surface ELISA (Figure S1). The deviation from the wt PrRPR surface expression levels (wt = 39.6 ± 1.1%) varies from 16.3% ($W^{5.28}$A) to 59.6% ($F^{6.54}$A/$D^{6.59}$A). However, these differences, basically resulting from transient transfection, reveal minor effects in the IP accumulation signalling assay set up, as the receptor mutant $F^{6.54}$A (20.9 ± 3.7%) shows reduced total surface expression levels (Figure S1B) but full wt like efficacy (Figure 5B/C). Additionally, all PrRPR mutants are properly exported to the cell surface in comparable amounts as the wt receptor (39.6%, Figure S1C). Therefore, the herein obtained results of potency of agonists at their receptor constructs do not result from altered expression or export levels.

A reduced efficacy was observed in the concentration-response dependent signal transduction assay for $W^{5.28}$A and $Y^{5.38}$A ($P<0.001$) and – with decreased impact – also for $E^{5.26}$A ($P<0.0094$, Figure 6C, Table 2). In summary, our findings support a binding mechanism in which $E^{5.26}$, in addition to $D^{6.59}$, directly engage $R^{19}$ of PrRP20 through ionic interactions. $F^{6.54}$ might contribute to the overall global conformation of the binding pocket and positioning of TMH 6, as its single mutation is less invasive but still is in distance for direct ligand interactions. We further suggest that $W^{5.28}$ and $Y^{5.38}$ are possibly in direct contact with the ligand and are indeed critical for receptor activation and the transmission of an external signal into the cell.

*Exploration of second interaction partner and dual binding mode at $R^{19}$.* We generated the $E^{5.26}$A/$D^{6.59}$A double mutant of the receptor, which lacks both putative binding partners to the $R^{19}$. In addition, the reciprocal PrRPR mutants, $E^{5.26}$R/$D^{6.59}$R and $E^{5.26}$R, were generated to test the interaction by swapping the putative binding residues. The $E^{5.26}$A and the $E^{5.26}$A/$D^{6.59}$A receptor mutants were investigated in a double cycle mutagenesis study, where they were stimulated with $A^{19}$PrRP20 and wt PrRP20 (Table 1, Figure 7A). The $E^{5.26}$A mutant stimulated with $A^{19}$PrRP20 resulted in a strongly increased $EC_{50}$-value higher than 10 µM, 21-fold shifted compared to PrRP20 stimulation (537 nM). The enhanced $EC_{50}$-value can be explained by the disruption of the second $R^{19}$ interaction to receptor residue $D^{6.59}$. Indeed, this effect agrees with a

similar impact of the $D^{6.59}A$ mutation (15-fold shifted; Table 1), which also diminished the direct interaction to the $R^{19}$ of the ligand to a similar extent (Figure 2A, 7A). Furthermore, the stimulation of the $E^{5.26}A/D^{6.59}A$ receptor mutant with either PrPR20 or $A^{19}$PrRP20 resulted in matching curves. As no additional loss in potency was observed compared to the $E^{5.26}A$ mutant tested with $A^{19}$PrRP20 (Figure 7B), the experiment provides evidence that $E^{5.26}$ is involved in binding to $R^{19}$.

Next, the capability of receptor mutants $E^{5.26}A$, $E^{5.26}A/D^{6.59}A$, $E^{5.26}R$, $E^{5.26}R/D^{6.59}R$, $D^{6.59}A$, and wt PrRPR to transmit signalling was tested (Figure 7E). Importantly, the reciprocal receptor mutants $E^{5.26}R$ and $E^{5.26}R/D^{6.59}R$ were significantly and best activated by $D^{19}$PrRP20 (both: $P<0.001$). In fact, $E^{5.26}R/D^{6.59}R$ was solely activated by $D^{19}$PrRP20. Finally, the $E^{5.26}R$ mutant was stimulated with PrRP20, $A^{19}$PrRP20, and $D^{19}$PrRP20 in a concentration-response experiment (Figure 7C). This receptor mutant behaved similarly, when stimulated by PrRP20 and $D^{19}$PrRP20 (both: $EC_{50}$-value >10 µM). Along with the experiments testing $D^{19}$PrRP20 stimulation of wt PrRPR, we demonstrate an approximately equal repulsive effect of $R^{19}$ to $E^{5.26}R$ or $D^{19}$ to $D^{6.59}$ (Figure 7D). This strengthens our hypothesis of a dual binding mode of $R^{19}$ to $E^{5.26}$ and $D^{6.59}$.

*Comparative model of PrRP/receptor complex provides structural information on mode of binding.* Using the $R^{19}/E^{5.26}$ and $R^{19}/D^{6.59}$ contacts as restraints, a *de novo*-folded model of PrRP8-20 based on reported NMR data (18) was docked into an ensemble of comparative models of the PrRPR. The conformation of the EL regions was constructed simultaneously with ligand docking to accurately capture conformational changes induced by the peptide. Details of the modeling procedures are given in the Materials and Methods and Supplemental Information. The lowest-energy ROSETTA model features salt bridges between $D^{6.59}$, $E^{5.26}$, and $R^{19}$. $W^{5.28}$ and $Y^{5.38}$ form π-stacking interactions that may be indicative of a "toggle-switch" mechanism (Figure 8A) (43). $F^{6.54}$ appears to further apart from $R^{19}$ but might contribute to the positioning of TMH 6 via intra-molecular interactions and is in distance for π-stacking interactions with the $F^{20}$ of PrRP20. Additional interactions between peptide and receptor hold the peptide in an optimal binding conformation deeply buried in the upper TMH segments and supported by the ELs from above.

## DISCUSSION

We have evolved a strategy to interrogate detailed molecular mechanisms of GPCR activation by combining reciprocal, double cycle, and intramolecular double mutagenesis with computational modelling. We apply this technique effectively to PrRPR and its CAM, $D^{6.59}R$ PrRPR, identifying distinct receptor residues involved in activation and/or ligand binding.

This is the first comprehensive mutational study of the extracellular and transmembrane regions of the PrRPR. The double cycle mutagenic approach suggests the interaction (direct or indirect) between residues $D^{6.59}$ and $R^{19}$ and provides a first anchor point for receptor/ligand investigations. Interacting residues can be characterized by reciprocal mutagenesis, as shown before in an intramolecular study with the $D^{2.61}R/R^{7.39}D$ swap in the gastrin-releasing peptide receptor (44) or the $D^{6.44}/N^{7.49}$ residues of the thyrotropin (TSH) receptor (45). By applying this method to the PrRP/PrRPR system, the salt bridge of $D^{6.59}$ to $R^{19}$ was verified, and more importantly, by generating the $D^{6.59}R$ receptor, we identified the first CAM of the PrRPR. Up to now, numerous CAM were generated and investigated in a plethora of previous studies, emphasizing the increasing importance of CAMs. For example, CAM of the human angiotensin II type 1 receptor with $N^{3.35}$Gly (46), the $ß_{1B}$ (47)/ $ß_2$-adrenergic receptor (48-50), the cannabinoid receptor 1 (51), muscarinic $m_1$ (52) and $m_5$ receptors (53) among others, have been found. Interestingly, more than sixty naturally occurring CAM GPCR are known so far (54) and are often related to human disorders (55). Consequently, GPCR activated in an agonist-independent manner are of emerging importance for drug development (3).

CAM more readily undergo transition between active and inactive conformations due to removed conformational constraints of the inactive form (56). Because $D^{6.59}R$ in PrRPR is located at the top of TMH6, we hypothesize that this helix is involved in receptor activation via an inward movement of the upper helical region (Figure 4D). Similarly to the PrRPR $D^{6.59}R$ CAM, mutant-

induced receptor activity was observed in the $S^{6.58}Y/T^{6.59}P$ double mutant of $m_5$ muscarinic receptors (57). These data indicate that the top of TMH6 is directly involved in the switch between the active and the inactive state of several GPCR and that the interaction with the ligand stabilizes the receptor in this active conformation – a notion that supports the "global toggle switch model" (58-60). This model suggests that activation results from an inward movement of the extracellular ends of TMHs 6 and 7 toward TMH3, concomitant with a movement of the intracellular part of the TMHs in the opposite direction, which enables signaling via G-protein coupling. PrRPR represents an excellent model system to further investigate this hypothesis and gain insights to receptor activating mechanisms.

Previous work on the TSH receptors showed the effects of spatially distant double mutants on constitutive activity (61-62). However, we focus on the investigation of the molecular vicinity surrounding $D^{6.59}$, as we suggest that specific inter-residue interactions of the generated CAM occur. To take advantage of the $D^{6.59}R$ CAM to elucidate the mechanism of ligand binding and PrRPR activation, we established an effective combination of intramolecular double and inter-molecular reciprocal mutagenic approaches to study PrRPR activation by wt PrRP20, $A^{19}$PrRP20, and $D^{19}$PrRP20. With guidance from the PrRPR comparative model, seven possible interacting residues were considered (Figure 5A), and the double mutants $E^{5.26}A/D^{6.59}R$, $W^{5.28}A/D^{6.59}R$, $Y^{5.38}A/D^{6.59}R$, and $F^{6.54}A/D^{6.59}R$ revealed an involvement of these residues in receptor activation. Importantly, these receptor mutants were significantly activated by $D^{19}$PrRP20 but not by wt PrRP20 (Fig. 5B), proving that the receptor mutants were not miss-folded and that $D^{19}$ on the ligand is still able to interact with $D^{6.59}R$. CAM are thought to mimic, at least partially, the active conformation of the wt receptor and to spontaneously adopt a structure able to activate G-proteins (63). Therefore, we hypothesize that in $D^{19}$PrRP20, residue $D^{19}$ takes over the role of the destroyed intra-molecular interaction of the double mutants, reactivating the "silenced" CAM. The conformation of a basally silenced GPCR might impair its intrinsic capacity for signaling compared to the wt receptor. Notably, further mutations within EL2/TMH5 had no considerable impact on receptor potency, in contrast to all three positions identified via intramolecular interactions (Table 2). This demonstrates the precision and usefulness of the modeling-guided double mutational approach to identify interacting residues in close proximity to the ligand.

In contrast, the $W^{2.71}A/D^{6.59}R$ control turned out to be deficient in signaling. This is expected and in agreement with the high conservation of $W^{2.70}/W^{2.71}$ in most peptide GPCR, e.g. in the NPY receptor system (14). Furthermore, $W^{2.71}$ is located in the structurally relevant WxGF-motif, which is suggested to be a key component in the activation mechanism in many GPCR in the rhodopsin family (64). Recent investigations on TMH2 of the CAM $N^{3.35}G$ hAT1 suggested TMH2 to pivot, bringing the top of TMH2 closer to the binding pocket (65). Our results obtained for the conserved $Y^{2.64}$ on top of TMH2 do not support such a spatial approach to $D^{6.59}$ and thus to the binding pocket. This reflects the divergence of GPCR activation and accentuates that the detailed mode of activation is not a common mechanism.

The results obtained from studies of the $E^{5.26}A$ mutation lead to the conclusion that this residue is predominantly responsible for ligand binding. Our initial double cycle mutagenic experiments at $D^{6.59}$ support a more complex double binding role for $R^{19}$ of PrRP20, which appears to be in contact with two sites on PrRPR. Accordingly, we suggest $E^{5.26}$ to be the second binding partner for peptide residue $R^{19}$ (Figure 7D). The extensive mutagenic studies of residue $E^{5.26}$ strongly indicate the participation in binding to $R^{19}$ and the constitutive activity of $D^{6.59}R$ supports the hypothesis of a second R-specific interaction site in PrRPR that can be satisfied by the $D^{6.59}R$ but not the $D^{6.59}K$ mutant. A similar dual binding mode for arginine was recently reported for gonadotropin-releasing hormone (GnRH) receptor (66). This has been supported by other studies, where substitution of $R^{19}$ to lysine, citruline (Cit), α-amino-4-guanidino-butyric acid (Agb), or α-amino-3-guanidino-propionic acid (Agp) on the peptide lead to reduced binding affinities (12). Interestingly, the tight ensemble of models that is in agreement with the experimental data presented herein exhibits variability in ELs 1 and 2 while still maintaining the contacts between $D^{6.59}$ and $E^{5.26}$ with $R^{19}$. Given this structural variability in our models, we emphasize that the

presented approach is an iterative process, where initial models can be used to guide experimental design, and the resulting data allow for model refinement. The current PrRP/receptor model can only be considered valid in the light of the functional data. However, it provides insight into possible structural mechanisms of peptide/receptor interactions and receptor activation.

$W^{5.28}A$ and $Y^{5.38}A$ also showed lowered ligand potency, but both mutants revealed a strongly decreased ability to transmit signals compared to the wt receptor (Table 2). This effect may result from intramolecular structural alteration due to the lack of aromaticity at the $Y^{5.38}A$ site. Mutational studies reported for the nearby $Y^{5.39}$ residue in both cannabinoid receptors ($CB_1$ and $CB_2$) revealed that the aromaticity at this position is crucial (67). The PrRP/receptor model places $W^{5.28}$ in close proximity to $Y^{5.38}$ (Figure 8A). In this model, the residues form stacking interactions, but this remains to be proven experimentally. We speculate that, due to the effects observed for potency and efficacy, $W^{5.28}$ and $Y^{5.38}$ are related to receptor activation. In contrast, $F^{6.54}A$ mutant reveals full wt efficacy accompanied with reduced potency. From the docked modeling data, we speculate that this residue contributes to the correct conformation of the binding pocket and might interact with the $F^{20}$ of the PrPR20.

Evolutionary and structural studies revealed that the PrRPR belongs to the family of RF-amide peptide receptors, consisting of five discovered groups: the neuropeptide FF (NPFF) group, the prolactin-releasing peptide (PrRP) group, the gonadotropin-inhibitory hormone (GnIH) group, the kisspeptin group, and the 26RFa group (68-70). However, further phylogenic investigations revealed that the PrPRR shares an ancient receptor with the NPY receptors (17). The human PrRPR possesses high sequence identity with the human $NPY_2R$, particularly in the upper and middle regions of TMH 4, TMH 5, and TMH 6. It is suggested that the PrRPR family began co-evolving with ancestral PrRP/C-RF-amide peptide with a redundant NPY binding receptor (17). This explains the importance of the conserved $D^{6.59}$ residue and in turn, might have been responsible for the development of a double binding mode for $R^{19}$ in the PrRPR/PrRP system. It could be speculated that other RF-amide receptors evolved similar binding modes for the crucial arginine within the RF-amide motif, especially for the closely related 26RF-amide receptor. In contrast, for the well investigated Y-receptor family, a double binding mode was not identified, neither for $R^{33}$ at $Y_2/Y_5R$ nor for $R^{35}$ at $Y_1/Y_4R$ (14-15). However, the second interaction might occur via the second arginine 33 or 35, respectively.

Regarding medical and physiological implications, the expression of CAM can entail oncogenic effects, such as tumor formation in nude mice (71). A variety of diseases are known to be triggered by elevated basal activity, including autosomal dominant hypocalcaemia (72) and ovarian hyperstimulation syndrome (73). Our findings provide insight into the harmful potential of CAM and demonstrate the need for applicable drugs that are able to diminish mutation-induced receptor activity. We are confident that our technique is a promising tool to investigate residues relevant for ligand binding and receptor activation because a CAM is used as a template. Our approach paves the way for obtaining specific structure/function information on a molecular level, which is of indispensible value, as no crystal structure for a peptide GPCR currently exists. This method will hopefully contribute to the elucidation of the structural mechanisms of harmful CAM and help to develop and increase the number of inverse-agonist drugs that target these receptors.

**REFERENCES**

1. Hopkins, A. L., and Groom, C. R. (2002) *Nat. Rev. Drug Discov.* **1**, 727-730
2. Lagerström, M. C., and Schiöth, H. B. (2008) *Nat. Rev. Drug Discov.* **7**, 339-357
3. Bond, R. A., and Ijzerman, A. P. (2006) *Trends Pharmacol. Sci.* **27**, 92-96
4. Welch, S. K., O'Hara, B. F., Kilduff, T. S., and Heller, H. C. (1995) *Biochem. Biophys. Res. Commun.* **209**, 606-613

5. Fujii, R., Fukusumi, S., Hosoya, M., Kawamata, Y., Habata, Y., Hinuma, S., Sekiguchi, M., Kitada, C., Kurokawa, T., Nishimura, O., Onda, H., Sumino, Y., and Fujino, M. (1999) *Regul. Pept.* **83**, 1-10
6. Langmead, C. J., Szekeres, P. G., Chambers, J. K., Ratcliffe, S. J., Jones, D. N., Hirst, W. D., Price, G. W., and Herdon, H. J. (2000) *Br. J. Pharmacol.* **131**, 683-688
7. Fukusumi, S., Fujii, R., and Hinuma, S. (2006) *Peptides* **27**, 1073-1086
8. Hinuma, S., Habata, Y., Fujii, R., Kawamata, Y., Hosoya, M., Fukusumi, S., Kitada, C., Masuo, Y., Asano, T., Matsumoto, H., Sekiguchi, M., Kurokawa, T., Nishimura, O., Onda, H., and Fujino, M. (1998) *Nature* **393**, 272-276
9. Lin, S. H. (2008) *Results Probl. Cell Differ.* **46**, 57-88
10. Boyle, R. G., Downham, R., Ganguly, T., Humphries, J., Smith, J., and Travers, S. (2005) *J. Pept. Sci.* **11**, 161-165
11. Roland, B. L., Sutton, S. W., Wilson, S. J., Luo, L., Pyati, J., Huvar, R., Erlander, M. G., and Lovenberg, T. W. (1999) *Endocrinology* **140**, 5736-5745
12. Danho, W., Swistok, J., Khan, W., Truitt, T., Kurylko, G., Fry, D., Greeley, D., Sun, H., Dvorozniak, M., Machie, G., Spence, C., and Goodnow, R. (2003) Structure-activity relationships and bioactive conformations of prolactine releasing peptides. Ligands for a potential obesity target. in *18th American Peptide Symposium* Kluwer Academic, Norwell, MA, Boston
13. Conner, A. C., Barwell, J., Poyner, D. R., and Wheatley, M. (2011) *Methods Mol. Biol.* **746**, 85-98
14. Lindner, D., van Dieck, J., Merten, N., Mörl, K., Günther, R., Hofmann, H. J., and Beck-Sickinger, A. G. (2008) *Biochemistry* **47**, 5905-5914
15. Merten, N., Lindner, D., Rabe, N., Römpler, H., Mörl, K., Schöneberg, T., and Beck-Sickinger, A. G. (2007) *J. Biol. Chem.* **282**, 7543-7551
16. Ballesteros, J. A., and Weinstein, H. (1995) *Methods Neurosci* **25**, 366-428
17. Lagerstrom, M. C., Fredriksson, R., Bjarnadottir, T. K., Fridmanis, D., Holmquist, T., Andersson, J., Yan, Y. L., Raudsepp, T., Zoorob, R., Kukkonen, J. P., Lundin, L. G., Klovins, J., Chowdhary, B. P., Postlethwait, J. H., and Schioth, H. B. (2005) *Genomics* **85**, 688-703
18. D'Ursi, A. M., Albrizio, S., Di Fenza, A., Crescenzi, O., Carotenuto, A., Picone, D., Novellino, E., and Rovero, P. (2002) *J. Med. Chem.* **45**, 5483-5491
19. Carter, P. J., Winter, G., Wilkinson, A. J., and Fersht, A. R. (1984) *Cell* **38**, 835-840
20. Krylov, D., Mikhailenko, I., and Vinson, C. (1994) *EMBO J* **13**, 2849-2861
21. Lang, M., Bufe, B., De Pol, S., Reiser, O., Meyerhof, W., and Beck-Sickinger, A. G. (2006) *J Pept Sci* **12**, 258-266
22. Findeisen, M., Rathmann, D., and Beck-Sickinger, A. G. (2011) *ChemMedChem* **6**, 1081-1093
23. Sanger, F., Nicklen, S., and Coulson, A. R. (1992) *Biotechnology* **24**, 104-108
24. Bohme, I., Stichel, J., Walther, C., Morl, K., and Beck-Sickinger, A. G. (2008) *Cell Signal* **20**, 1740-1749
25. Reynolds, C. P., Biedler, J. L., Spengler, B. A., Reynolds, D. A., Ross, R. A., Frenkel, E. P., and Smith, R. G. (1986) *J Natl Cancer Inst* **76**, 375-387
26. Höfliger, M. M., Castejon, G. L., Kiess, W., and Beck Sickinger, A. G. (2003) *J. Recept. Signal. Transduct. Res.* **23**, 351-360

27. Böhme, I., Mörl, K., Bamming, D., Meyer, C., and Beck-Sickinger, A. G. (2007) *Peptides* **28**, 226-234
28. Koglin, N., Lang, M., Rennert, R., and Beck-Sickinger, A. G. (2003) *J. Med. Chem.* **46**, 4369-4372
29. Thompson, J. D., Higgins, D. G., and Gibson, T. J. (1994) *Nucleic Acids Res* **22**, 4673-4680
30. Konagurthu, A. S., Whisstock, J. C., Stuckey, P. J., and Lesk, A. M. (2006) *Proteins* **64**, 559-574
31. Okada, T., Sugihara, M., Bondar, A.-N., Elstner, M., Entel, P., and Buss, V. (2004) *Journal of Molecular Biology* **342**, 571-583
32. Park, J. H., Scheerer, P., Hofmann, K. P., Choe, H.-W., and Ernst, O. P. (2008) *Nature* **454**, 183-187
33. Scheerer, P., Park, J. H., Hildebrand, P. W., Kim, Y. J., Krauß, N., Choe, H.-W., Hofmann, K. P., and Ernst, O. P. (2008) *Nature* **455**, 497-502
34. Cherezov, V., Rosenbaum, D. M., Hanson, M. A., Rasmussen, S. G. F., Thian, F. S., Kobilka, T. S., Choi, H.-J., Kuhn, P., Weis, W. I., Kobilka, B. K., and Stevens, R. C. (2007) *Science* **318**, 1258-1265
35. Warne, T., Serrano-Vega, M. J., Baker, J. G., Moukhametzianov, R., Edwards, P. C., Henderson, R., Leslie, A. G. W., Tate, C. G., and Schertler, G. F. X. (2008) *Nature* **454**, 486-491
36. Jaakola, V.-P., Griffith, M. T., Hanson, M. A., Cherezov, V., Chien, E. Y. T., Lane, J. R., Ijzerman, A. P., and Stevens, R. C. (2008) *Science* **322**, 1211-1217
37. Mandell, D. J., Coutsias, E. A., and Kortemme, T. (2009) *Nat Meth* **6**, 551-552
38. Canutescu, A., and Dunbrack Jr, R. (2003) *Protein Science: A Publication of the Protein Society* **12**, 963
39. Barth, P., Schonbrun, J., and Baker, D. (2007) *Proc Natl Acad Sci U S A* **104**, 15682-15687
40. Gray, J. J., Moughon, S., Wang, C., Schueler-Furman, O., Kuhlman, B., Rohl, C. A., and Baker, D. (2003) *J Mol Biol* **331**, 281-299
41. Rohl, C. A. (2005) *Methods in enzymology* **394**, 244-260
42. Madsen, K. L., Thorsen, T. S., Rahbek-Clemmensen, T., Eriksen, J., and Gether, U. (2012) *The Journal of biological chemistry* **287**, 12293-12308
43. Nygaard, R., Frimurer, T. M., Holst, B., Rosenkilde, M. M., and Schwartz, T. W. (2009) *Trends Pharmacol Sci* **30**, 249-259
44. Donohue, P. J., Sainz, E., Akeson, M., Kroog, G. S., Mantey, S. A., Battey, J. F., Jensen, R. T., and Northup, J. K. (1999) *Biochemistry* **38**, 9366-9372
45. Govaerts, C., Lefort, A., Costagliola, S., Wodak, S. J., Ballesteros, J. A., Van Sande, J., Pardo, L., and Vassart, G. (2001) *J Biol Chem* **276**, 22991-22999
46. Arsenault, J., Cabana, J., Fillion, D., Leduc, R., Guillemette, G., Lavigne, P., and Escher, E. (2010) *Biochem Pharmacol* **80**, 990-999
47. Scheer, A., Fanelli, F., Costa, T., De Benedetti, P. G., and Cotecchia, S. (1996) *EMBO J* **15**, 3566-3578
48. Lefkowitz, R. J., Cotecchia, S., Samama, P., and Costa, T. (1993) *Trends in pharmacological sciences* **14**, 303-307
49. Lefkowitz, R. J., Cotecchia, S., Samama, P., and Costa, T. (1993) *Trends Pharmacol. Sci.* **14**, 303-307

50. Samama, P., Cotecchia, S., Costa, T., and Lefkowitz, R. J. (1993) *J. Biol. Chem.* **268**, 4625-4636
51. D'Antona, A. M., Ahn, K. H., Wang, L., Mierke, D. F., Lucas-Lenard, J., and Kendall, D. A. (2006) *Brain Res* **1108**, 1-11
52. Högger, P., Shockley, M. S., Lameh, J., and Sadee, W. (1995) *J Biol Chem* **270**, 7405-7410
53. Spalding, T. A., Burstein, E. S., Brauner-Osborne, H., Hill-Eubanks, D., and Brann, M. R. (1995) *J Pharmacol Exp Ther* **275**, 1274-1279
54. Seifert, R., and Wenzel-Seifert, K. (2002) *Naunyn Schmiedebergs Arch Pharmacol* **366**, 381-416
55. Spiegel, A. M. (1996) *Annu Rev Physiol* **58**, 143-170
56. Gether, U., Ballesteros, J. A., Seifert, R., Sanders-Bush, E., Weinstein, H., and Kobilka, B. K. (1997) *J Biol Chem* **272**, 2587-2590
57. Ford, D. J., Essex, A., Spalding, T. A., Burstein, E. S., and Ellis, J. (2002) *J Pharmacol Exp Ther* **300**, 810-817
58. Schwartz, T. W., Frimurer, T. M., Holst, B., Rosenkilde, M. M., and Elling, C. E. (2006) *Annu Rev Pharmacol Toxicol* **46**, 481-519
59. Schwartz, T. W., Frimurer, T. M., Holst, B., Rosenkilde, M. M., and Elling, C. E. (2006) *Annu. Rev. Pharmacol. Toxicol.* **46**, 481-519
60. Elling, C. E., Frimurer, T. M., Gerlach, L. O., Jorgensen, R., Holst, B., and Schwartz, T. W. (2006) *J. Biol. Chem.* **281**, 17337-17346
61. Kleinau, G., Jaeschke, H., Mueller, S., Worth, C. L., Paschke, R., and Krause, G. (2008) *Cell Mol Life Sci* **65**, 3664-3676
62. Gruters, A., Schoneberg, T., Biebermann, H., Krude, H., Krohn, H. P., Dralle, H., and Gudermann, T. (1998) *J Clin Endocrinol Metab* **83**, 1431-1436
63. Cotecchia, S., Fanelli, F., and Costa, T. (2003) *Assay Drug Dev Technol* **1**, 311-316
64. Klco, J. M., Nikiforovich, G. V., and Baranski, T. J. (2006) *J Biol Chem* **281**, 12010-12019
65. Domazet, I., Holleran, B. J., Martin, S. S., Lavigne, P., Leduc, R., Escher, E., and Guillemette, G. (2009) *J Biol Chem* **284**, 11922-11929
66. Flanagan, C. A., Rodic, V., Konvicka, K., Yuen, T., Chi, L., Rivier, J. E., Millar, R. P., Weinstein, H., and Sealfon, S. C. (2000) *Biochemistry* **39**, 8133-8141
67. McAllister, S. D., Tao, Q., Barnett-Norris, J., Buehner, K., Hurst, D. P., Guarnieri, F., Reggio, P. H., Nowell Harmon, K. W., Cabral, G. A., and Abood, M. E. (2002) *Biochem Pharmacol* **63**, 2121-2136
68. Ukena, K., Vaudry, H., Leprince, J., and Tsutsui, K. (2011) *Cell Tissue Res* **343**, 475-481
69. Osugi, T., Ukena, K., Sower, S. A., Kawauchi, H., and Tsutsui, K. (2006) *FEBS J* **273**, 1731-1743
70. Findeisen, M., Rathmann, D., and Beck-Sickinger, A. G. (2011) *Pharmaceuticals* **4**, 1248-1280
71. Allen, L. F., Lefkowitz, R. J., Caron, M. G., and Cotecchia, S. (1991) *P Natl Acad Sci USA* **88**, 11354-11358
72. Okazaki, R., Chikatsu, N., Nakatsu, M., Takeuchi, Y., Ajima, M., Miki, J., Fujita, T., Arai, M., Totsuka, Y., Tanaka, K., and Fukumoto, S. (1999) *J Clin Endocrinol Metab* **84**, 363-366

73. Gromoll, J., Simoni, M., Nordhoff, V., Behre, H. M., De Geyter, C., and Nieschlag, E. (1996) *Mol Cell Endocrinol* **125**, 177-182

*Acknowledgments*-The authors thank Kristin Löbner and Christina Dammann for their technical assistance in peptide synthesis, Janet Schwesinger for sequencing, and Regina Reppich-Sacher for recording mass spectra. They would also like to thank members of the ROSETTACOMMONS, Elizabeth Dong, David Nannemann, Steven Combs, and Anette Kaiser for their assistance and insight provided concerning the molecular modelling.

**FOOTNOTES**

*This work was financially supported by DFG to ABS (SFB 610, BE 1264-11) and NIH to JM (R01 MH090192, R01 GM GM080403).

[1]To whom correspondence may be addressed: Institute of Biochemistry, Universität Leipzig, Brüderstrasse 34, 04103 Leipzig, Germany. Tel.: +49 3419736901; Fax: +49 3419736909;
E-mail: beck-sickinger@uni-leipzig.de
[2]Center for Structural Biology, Vanderbilt University, TN465 21st Ave South, BIOSCI/MRBIII, Nashville, USA.
[3]Present address: Department of Cardiology and Pneumology, Charité, Universititäts-Medizin Berlin, Campus Benjamin Franklin, Hindenburgdamm 30, 12200 Berlin, Germany.
[4]These authors contributed equally to this work.

[5]The abbreviations used are: PrRPR, Prolactin releasing peptide receptor; wt, wild-type; GPCR, G-protein coupled receptor; CAM, constitutively active mutant; YR, Y-receptor; NPY, neuropeptide Y; IP, inositole phosphate; CCD, cyclic coordinate descent; eYFP, enhanced yellow fluorescence protein; EL, extracellular loop; TMH, transmembrane helix; TSH, thyrotropin; GnRH, gonadotropin-releasing hormone; CB, cannabinoid; NPFF, neuropeptide FF.
[6]Manuscript in preparation: S. H. DeLuca, D. Rathmann, A.G. Beck-Sickinger, J. Meiler.

## FIGURE LEGENDS

FIGURE 1. **Identification of the conserved $D^{6.59}$ residue in the hPrRPR sequence as potential spot of interaction.** A. Conservation of $D^{6.59}$ shown in the amino acid sequence alignment. The region of upper transmembrane helix (TMH) 6 and the beginning of the subsequent extracellular loop (EL) 3 of the four human Y receptor subtypes and the PrRPR is presented. Sequence alignment and description was taken from: http://www.gpcr.org/7tm/. B. Comparison of the C-terminal amino acids of the Y receptor ligands and the PrRP20. C. Snake plot representing the sequence of the human PrRPR. Residues highlighted in black were investigated as double mutants in the $D^{6.59}$R construct. Selective alanine-scan was performed on residues pictured in grey, resulting in no functional alteration. Residues with white letters in grey correspond to the X.50 nomenclature (16). D. IP accumulating signal transduction assay performed for 1h with COS-7 cells in a concentration-response dependent manner reveals an impact of $D^{6.59}$A PrRPR in comparison to the wt PrRP receptor. Data represent the mean ± s.e.m. of multiple independent experiments (n = 32 for hPrRPR, and n = 12 for $D^{6.59}$A PrRPR). Receptor activity is expressed as percentage of the full response of PrRP20 at the wt PrRP receptor.

FIGURE 2. **Functional characterization of PrRP receptor mutant $D^{6.59}$A with PrRP20 and the modified ligand $A^{19}$PrRP20.** Schemes representing the postulated mode of ligand binding. Due to the different relevance of $D^{6.59}$ and the $R^{19}$, a second contact point for $R^{19}$ can be assumed. Complementary mutagenesis approach was used in combination with the signal transduction assay on cells, expressing the wt PrRPR or the $D^{6.59}$A mutant in order to observe concentration-response curves. Data represent the mean ± s.e.m. of multiple independent experiments (n = 32 for hPrRPR with PrRP20, n = 12 for $D^{6.59}$A PrRPR with PrRP20, n = 11 for hPrRPR with $A^{19}$PrRP20, and n = 3 for $D^{6.59}$A PrRPR with $A^{19}$PrRP20). Receptor activity is expressed as percentage of full PrRP20 response at the wt PrRP receptor. A. Modification of receptor side: $D^{6.59}$A PrRPR in comparison with wt receptor was stimulated with PrRP20. B. Exploring the ligand side: both PrRP20 and $A^{19}$PrRP20 were investigated using wt PrRPR. C. Complementary approach: $A^{19}$PrRP20 stimulation of wt and mutant receptor resulted almost matching concentration-response curves, indicating an interaction between $D^{6.59}$ of the receptor and $R^{19}$ of the ligand.

FIGURE 3. **Reciprocal mutagenesis of the PrRPR.** A. This scheme displays the assumed wt situation with the direct interaction of ligand $R^{19}$PrRP20 and receptor $D^{6.59}$PrRPR, as well as the second unknown interaction of the $R^{19}$ to the receptor. B. The stimulation of wt receptor by $D^{19}$PrRP20 and the corresponding concentration-response curves of the signal transduction assay. C. Reciprocal mutagenesis scheme is shown with related concentration-response curves. Interestingly, $D^{6.59}$R mutant is partially basally active and can be activated by $D^{19}$PrRP20. The latter is due to the established D-R interaction. IP accumulation presented in panels B and C represent the mean ± s.e.m. of multiple independent experiments (n = 32 for hPrRPR with PrRP20, n = 5 for $D^{6.59}$R PrRPR with PrRP20, n = 4 for hPrRPR with $D^{19}$PrRP20, and n = 3 for $D^{6.59}$R PrRPR with $D^{19}$PrRP20). Receptor activity is expressed as percentage of full PrRP20 response at the wt PrRP receptor.

FIGURE 4. **Investigation of the constitutive activity of $D^{6.59}$R PrRPR mutant.** A. Test of influence of transfection upon constitutive activity of wt PrRPR and $D^{6.59}$ constructs. The IP accumulation of differently transient transfected COS-7 cells expressing the various PrRPR mutants was measured without any agonist after three hours [given as x-fold over eYFP expressing cells]. [Each bar represents the mean ± s.e.m. of two different experiments; at least in triplicates; * $P < 0.05$; ** $P < 0.01$; *** $P < 0.001$] B. Constitutive activity of wt PrRPR and $D^{6.59}$ mutant was investigated in a time-dependent manner. The IP accumulation of COS-7 cells expressing the different PrRPR variants was measured without any agonist after different time periods [given as x-fold over eYFP expressing cells]. C. Concentration-response curves of D6.59 PrRP receptor munats. Data represent the mean ± s.e.m. of multiple independent experiments (n = 5 for hPrRPR, n = 4 for $D^{6.59}$A PrRPR, n = 3 for $D^{6.59}$R PrRPR,

and n = 2 for $D^{6.59}$K PrRPR). Receptor activity is expressed as percentage of full PrRP20 response at the wt PrRP receptor. D. Scheme of assumed explanation for the agonist-independent activity of the $D^{6.59}$R receptor mutant: We postulate that the $D^{6.59}$R is a CAM because $D^{6.59}$R mimics $R^{19}$ of PrRP20 by intra-molecular interaction with a receptor region "X," inducing a partially active receptor conformation.

FIGURE 5. **Molecular model of the PrRPR based on 3DQB and resulting double mutations based on the $D^{6.59}$R PrRPR construct.** A. Residues in proximity to the extracellular side are shown in purple. These were investigated in double mutational analysis with $D^{6.59}$R PrRPR. The $D^{6.59}$ on top of TMH4 is colored in blue, and the suggested inward movement of the extracellular helical part of TMH6 is indicated by an orange dart. B. A new approach to identify the missing interaction site, "X," arose by insertion of a second alanine substitution of assumed interacting residues to the $D^{6.59}$R PrRPR. The second mutation is expected to diminish the basal activity but retain the capability to be activated by $D^{19}$PrRP20. IP accumulation assay of COS-7 cells transfected with eYFP as control and the following constructs of PrRPR: wt, $D^{6.59}$R, $Y^{2.64}$A/$D^{6.59}$R, $W^{2.71}$A/$D^{6.59}$R, $E^{5.26}$A/$D^{6.59}$R, $W^{5.28}$A/$D^{6.59}$R, $Y^{5.38}$A/$D^{6.59}$R, $F^{6.54}$A/$D^{6.59}$R, $Q^{7.35}$A/$D^{6.59}$R, respectively. Incubation was performed for three hours without ligand, PrRP20 or $D^{19}$PrRP20, and results are presented in IP accumulation as percentage of full PrRP20 response at the wt PrRP receptor. [Each bar represents the mean ± s.e.m. of at least duplicates of four different experiments; ** $P < 0.01$; *** $P < 0.001$].

FIGURE 6. **Functional characterisation of PrRPR mutants with impact on receptor activation and ligand binding.** A. COS-7 cells transfected with wt PrRPR or $E^{5.26}$A/$D^{6.59}$R, $W^{5.28}$A/$D^{6.59}$R, $Y^{5.38}$A/$D^{6.59}$R, $F^{6.54}$A/$D^{6.59}$R receptor mutants, were stimulated for three hours with different $D^{19}$PrRP20 concentrations using a signal transduction assay. Data represent the mean ± s.e.m. of 5 (PrRPR), 3 ($E^{5.26}$A/$D^{6.59}$R, $W^{5.28}$A/$D^{6.59}$R, $Y^{5.38}$A/$D^{6.59}$R) or 2 ($F^{6.54}$A/$D^{6.59}$R) independent experiments, measured in duplicate. B. COS-7 cells transfected with wt (n = 32) and $E^{5.26}$A (n = 8), $W^{5.28}$A (n = 7), $Y^{5.38}$A (n = 5), $D^{6.59}$A (n = 12), and $F^{6.54}$A (n =3) PrRPR mutants, respectively, were investigated in signal transduction assay, and data are presented in concentration-response curves as percentage of full PrRP20 response at wt PrRP receptor. Stimulation was performed for 1 hour. The height of the curves correlates with the efficacy of the mutants. Potency is given by the degree of shift to the right and its resulting $EC_{50}$ value. C. COS-7 cells transfected with the mentioned constructs in panel B were incubated for one hour in a signal transduction assay with $1x10^{-5}$M (mutants) or $1x10^{-7}$M (wt) PrRP20, and without stimulus. Results are expressed as percentage of IP accumulation compared to the PrRPR, with lowest mean of value being 0% and highest 100%. [bars represent the mean ± s.e.m of duplicates of at least 3 different experiments; * $P < 0.05$; *** $P < 0.001$].

FIGURE 7. **Stimulation analysis of $E^{5.26}$ mutants reveals a preferential activation of R mutants by the reciprocal ligand $D^{19}$PrRP20.** Functional investigation of PrRPR mutants $E^{5.26}$A, $E^{5.26}$R, and $E^{5.26}$A/$D^{6.59}$A with the ligands PrRP20, $A^{19}$PrRP20, or $D^{19}$PrRP20. The signal transduction assay was performed in COS-7 cells expressing the wt PrRPR or $E^{5.26}$A, $E^{5.26}$R, or $E^{5.26}$A/$D^{6.59}$A mutants to observe concentration-response curves. Results of two independent experiments, each performed in duplicate, are presented as mean ± s.e.m of duplicates. A. $E^{5.26}$A PrRPR was stimulated with both PrRP20 and $A^{19}$PrRP20 and demonstrated an equipotent loss in potency compared to the $D^{6.59}$A PrRPR mutation (Figure 2A). Additionally, this panel highlights the direct interaction between $R^{19}$ and $D^{6.59}$. B. Stimulation with of the $E^{5.26}$A/$D^{6.59}$A receptor with $A^{19}$PrRP20 or PrRP20 revealed no further loss in potency and a slightly decreased efficacy compared to the $E^{5.26}$A PrRPR. This indicates that $E^{5.26}$ might be the second binding partner of $R^{19}$. C. Functional characterization of the reciprocal $E^{5.26}$R PrRPR mutant using $R^{19}$-modified PrRP20 analogues. D. The scheme shows the assumed interplay of attraction and repulsion for the reciprocal interaction of the ligands $R^{19}$PrRP20 and $D^{19}$PrRP20 with the $E^{5.26}$R PrRP receptor mutant from panel C. E. IP accumulation assay of COS-7 cells transfected with eYFP as control and the following constructs of PrRPR: wt, $E^{5.26}$A, $E^{5.26}$A/$D^{6.59}$A, $E^{5.26}$R, $E^{5.26}$R/$D^{6.59}$R, $D^{6.59}$R, respectively. Incubation was performed for one hour using 100 µM of PrRP20, $D^{19}$PrRP20, $A^{19}$PrRP20,

and without ligand. [Each bar represents the mean ± s.e.m. of at least duplicates of 2 different experiments; *** $P < 0.001$].

FIGURE 8. **Comparative model of PrRPR docked to the thirteen C-terminal residues of PrRP20.** A. Selected comparative model generated by ROSETTA in the presence of the PrRP ligand to support experimental data. The same color code used in Figure 5A is used here. The figure displays an ensemble of low-energy PrRP/receptor models generated in ROSETTA, that agrees well with experimental data. Residue $D^{6.59}$ is colored in blue, the peptide is presented in yellow, and residues in vicinity to PrRP are in purple. B. The eight non-redundant low-energy comparative models of the PrRP/receptor complex. These eight models were generated in the presence of structural constraints derived from the mutagenesis data described (see main text) and are considered energetically favorable according to the ROSETTA v3 all-atom scoring function. The peptide is highlighted in yellow, $D^{6.59}$ of the receptor in blue, EL1 of the receptor in green, and EL2 of the receptor in magenta.

## TABLES

**Table 1: Functional characterization of wildtype and $D^{6.59}$ PrRP receptor mutants with different PrRP analogs.** IP accumulating signal transduction assay was performed for 1 hour with different concentrations of modified PrRP20 peptides to determine $EC_{50}$-values from concentration-response curves.

| PrRPR mutants | PrRP20 | | | | $A^{19}$PrRP20 | | | $D^{19}$PrRP20 | |
|---|---|---|---|---|---|---|---|---|---|
| | $EC_{50}$ [nM][a] ($pEC_{50}$ ± SEM) | $EC_{50}$-ratio[b] (mut/wt) | Emax ± SEM [%][c] | N | $EC_{50}$ [nM][a] ($pEC_{50}$ ± SEM) | $EC_{50}$-ratio[b] (analog/wt) | N | $EC_{50}$ [nM][a] ($pEC_{50}$ ± SEM) | N |
| wt | 1.66 (8.78 ± 0.04) | 1 | 100 | 32 | 1202 (5.92 ± 0.08) | 736 | 11 | 1318 (5.88 ± 0.12) | 5 |
| $D^{6.59}A$ | 26 (7.59 ± 0.15) | 15 | 98 ± 7 | 12 | **166 (6.78 ± 0.17)** | **0.16** | 3 | 6456 (5.19 ± 0.16) | 4 |
| $D^{6.59}R$ | ND[d] | ND[e] | 60 ± 13 | 4 | > 10 000 (< 5) | ND[e] | 2 | **138 (6.86 ± 0.23)** | 3 |
| $D^{6.59}K$ | 1380 (5.86 ± 0.20) | 847 | 90 ± 10 | 3 | NT | - | - | **115 (6.94 ± 0.17)** | 2 |
| $D^{6.59}E$ | 3.98 (8.4 ± 0.19) | 2 | 106 ± 10 | 2 | NT | - | - | NT | - |
| $D^{6.59}N$ | 36.3 (7.44 ± 0.25) | 22 | 105 ± 20 | 2 | NT | - | - | NT | - |
| $E^{5.26}A$ | 537 (6.27 ± 0.09) | 361 | 81 ± 6 | 8 | > 10 000 (< 5) | 21 | 3 | NT | - |
| $E^{5.26}R$ | > 10 000 (< 5) | ND[e] | 70 ± 6 | 2 | ND[d] | ND[e] | 2 | > 10 000 (< 5) | 2 |
| $E^{5.26}A$/ $D^{6.59}A$ | ND[d] | ND[e] | 58 ± 7 | 2 | ND[d] | ND[e] | 2 | NT | - |
| $E^{5.26}R$/ $D^{6.59}R$ | NR | ND[e] | 8 ± 2 | 2 | NR | ND[e] | 2 | ND[d] | 2 |

NT represents not tested, NR indicates no response after stimulation with 10 µM and N displays the number of individual experiments.

[a] $EC_{50}$-/$pEC_{50}$-values were calculated from the mean ± s.e.m. of N independent experiments, measured in dublicate.

[b] Efficacy was determined as percentage compared to full PrRP20 response at wt

[c] The ratio was determined using the prism 5.03 global fitting function for $EC_{50}$ shift determination.

[d] ND, not determined because of lack of efficacy. The plateau of the curve was not reached.

[e] ND, not determinable.

**Table 2:** *Signal transduction of selected alanine of PrRP receptor mutants from extracellular loop 2 and top TMH5.* IP accumulating signal transduction assay was performed for 1 hour with different concentrations of modified PrRP20 peptides to determine $EC_{50}$-values from concentration-response curves.

| PrRPR mutant | $E_{max}$ ± SEM [%] [a] | *P* [b] | $pEC_{50}$ ± SEM[c] | $EC_{50}$ [nM][c] | $EC_{50}$-ratio (mut/wt)[d] | N |
|---|---|---|---|---|---|---|
| Wt | 100 | - | 8.78 ± 0.04 | 1.66 | 1 | 32 |
| $Y^{4.65}A$ | 63 ± 22 | ns | 8.03 ± 0.32 | 9.3 | 6 | 2 |
| $E^{4.68}A$ | 93 ± 8 | ns | 8.19 ± 0.19 | 6.4 | 4 | 3 |
| $K^{4.70}A$ | 111 ± 35 | ns | 8.41 ± 0.41 | 3.9 | 2 | 2 |
| $D^{4.73}A$ | 146 ± 41 | ns | 8.75 ± 0.49 | 1.78 | 1 | 2 |
| $R^{4.75}A$ | 87 ± 15 | ns | 8.32 ± 0.37 | 4.8 | 3 | 3 |
| $E^{5.25}A$ | 124 ± 10 | ns | 7.99 ± 0.13 | 10 | 6 | 3 |
| **$E^{5.26}A$** | **81 ± 5** | **0.0094** | **6.26 ± 0.10** | **549** | **331** | **8** |
| $F^{5.27}A$ | 122 ± 50 | ns | 8.14 ± 0.49 | 7.2 | 4 | 2 |
| **$W^{5.28}A$** | **48 ± 5** | **< 0.0001** | **6.02 ± 0.14** | **954** | **580** | **7** |
| $E^{5.32}A$ | 114 ± 11 | ns | 8.62 ± 0.14 | 2.4 | 1 | 2 |
| $R^{5.33}A$ | 115 ± 15 | ns | 8.57 ± 0.20 | 2.7 | 2 | 2 |
| $R^{5.35}A$ | 81 ± 4 | 0.0122 | 8.35 ± 0.32 | 4.5 | 3 | 2 |
| **$Y^{5.38}A$** | **46 ± 6** | **< 0.0001** | **6.99 ± 0.14** | **102** | **61** | **5** |
| $W^{5.40}A$ | 101 ± 38 | ns | 8.78 ± 0.49 | 1.7 | 1 | 2 |
| **$D^{6.59}A$** | **97 ± 6** | **ns** | **7.59 ± 0.15** | **26** | **15** | **12** |
| **$F^{6.54}A$** | **101 ± 3** | **ns** | **7.61 ± 0.10** | **25** | **15** | **3** |

N represents the number of independent experiments.
[a] Efficacy was determined as percentage compared to full PrRP20 response at wt.
[b] Significance *P* was estimated using the unpaired t-test (ns represents no significantly different means with $P \geq 0.05$).
[c] $EC_{50}$-/$pEC_{50}$-values were calculated from the mean ± s.e.m. of N independent experiments, measured in dublicate.
[d] The ratio was determined using the prism 5.03 function of dose-response EC50 shift determination by global fitting.

Figure 1

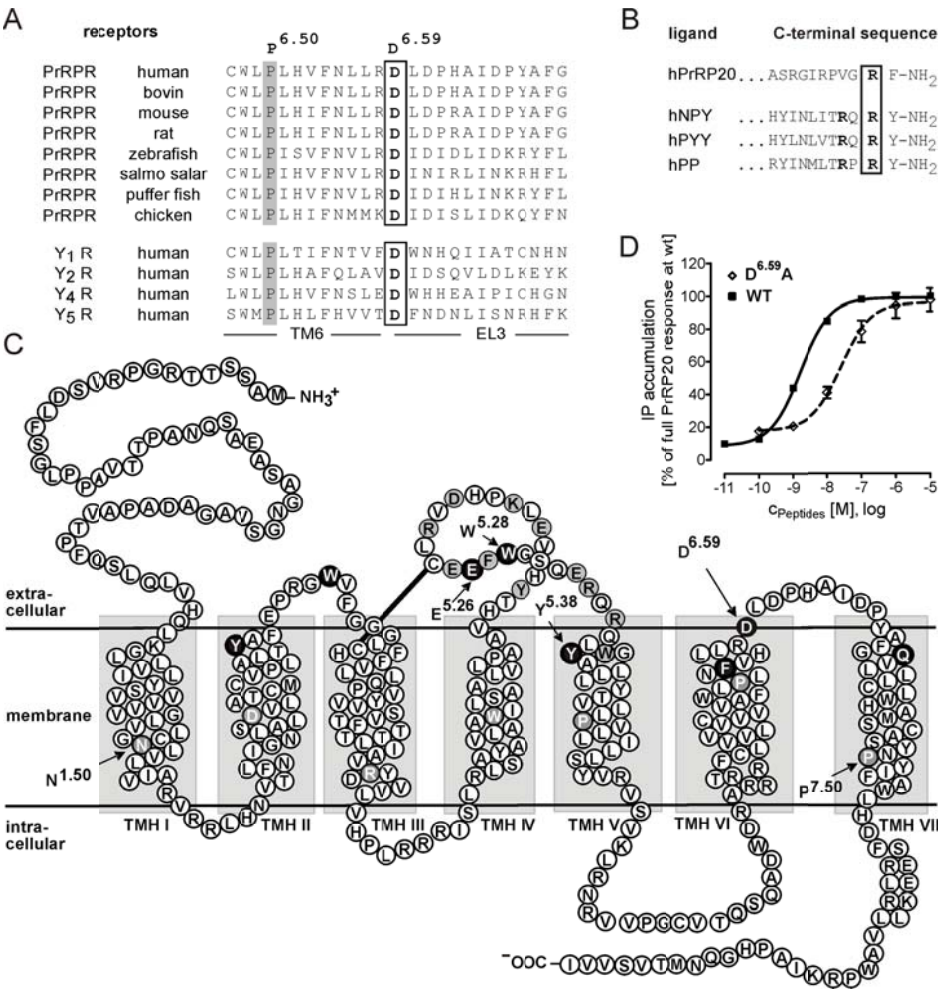

Figure 2

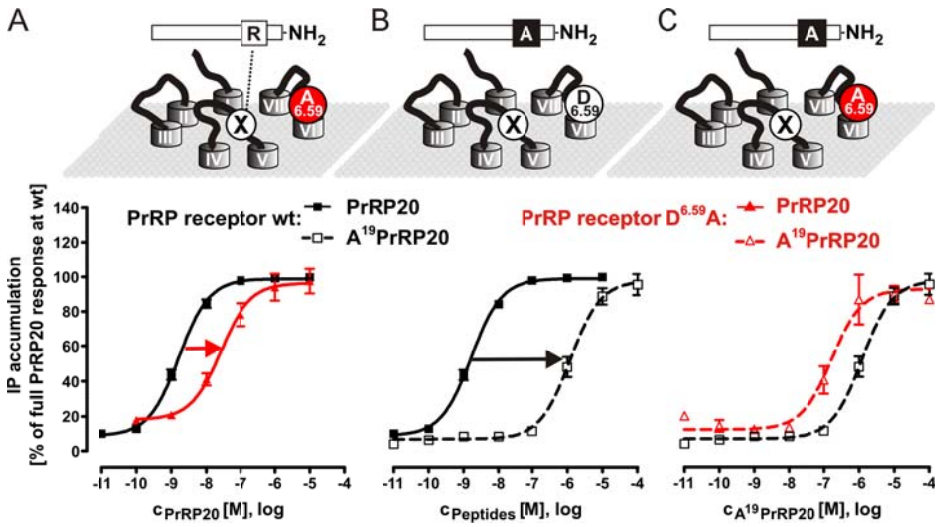

Figure 3

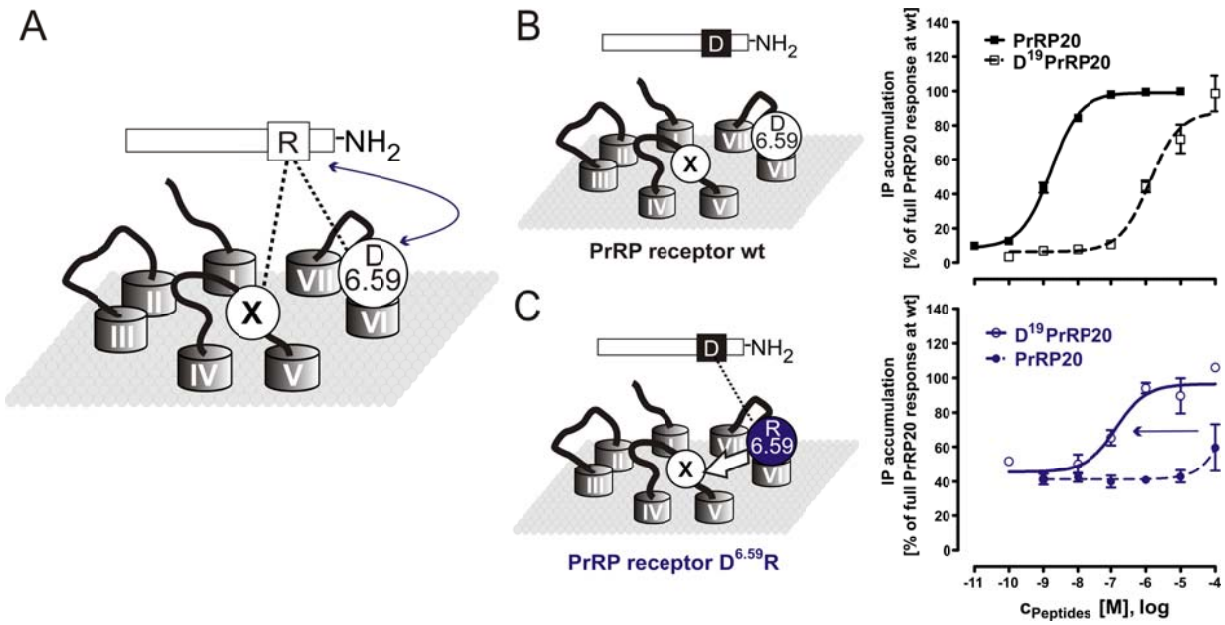

Figure 4

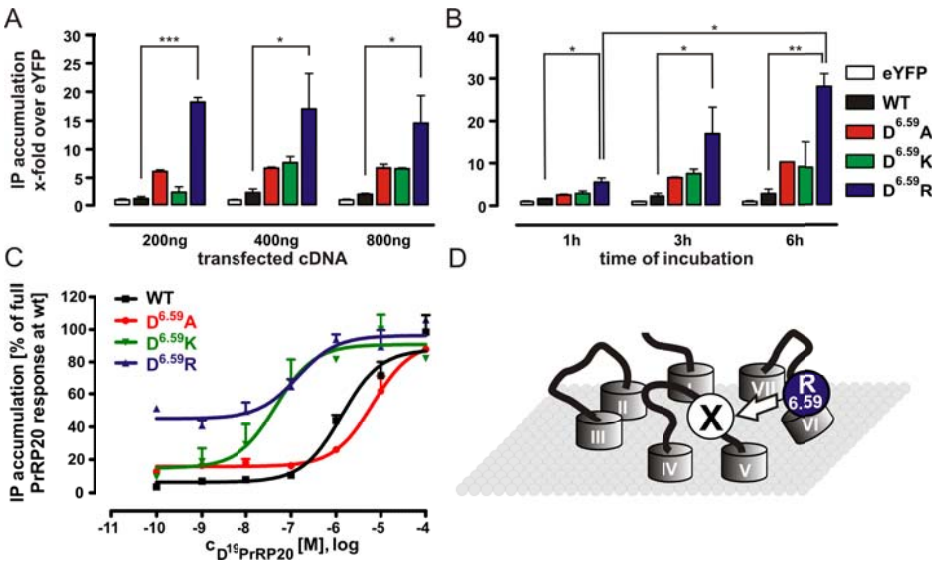

Figure 5

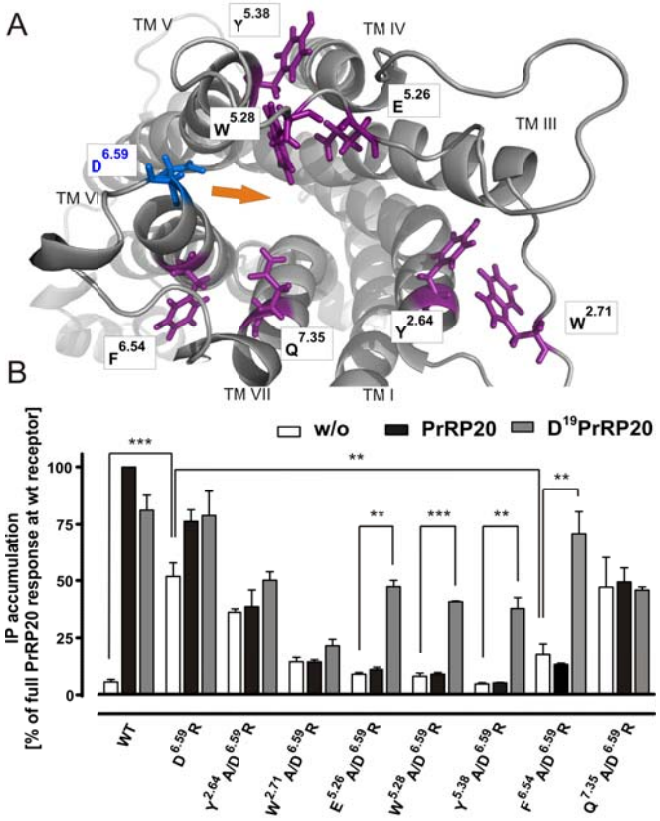

Figure 6

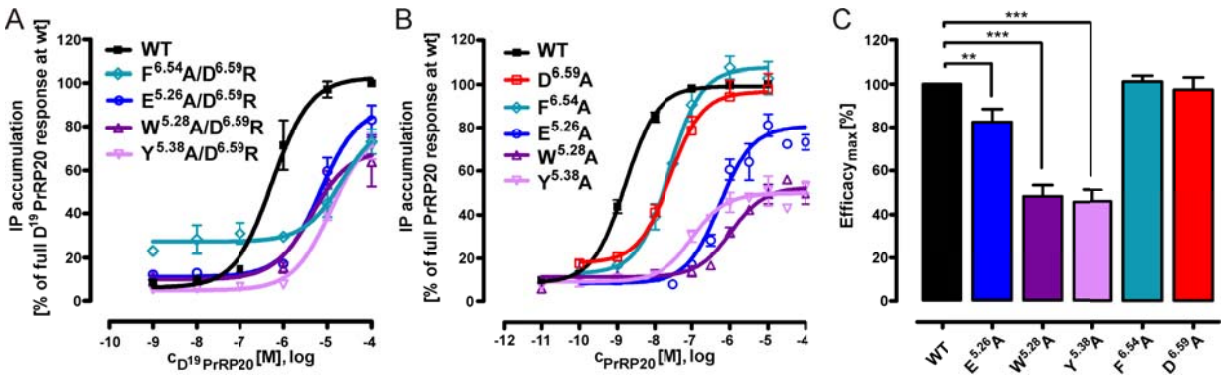

Figure 7

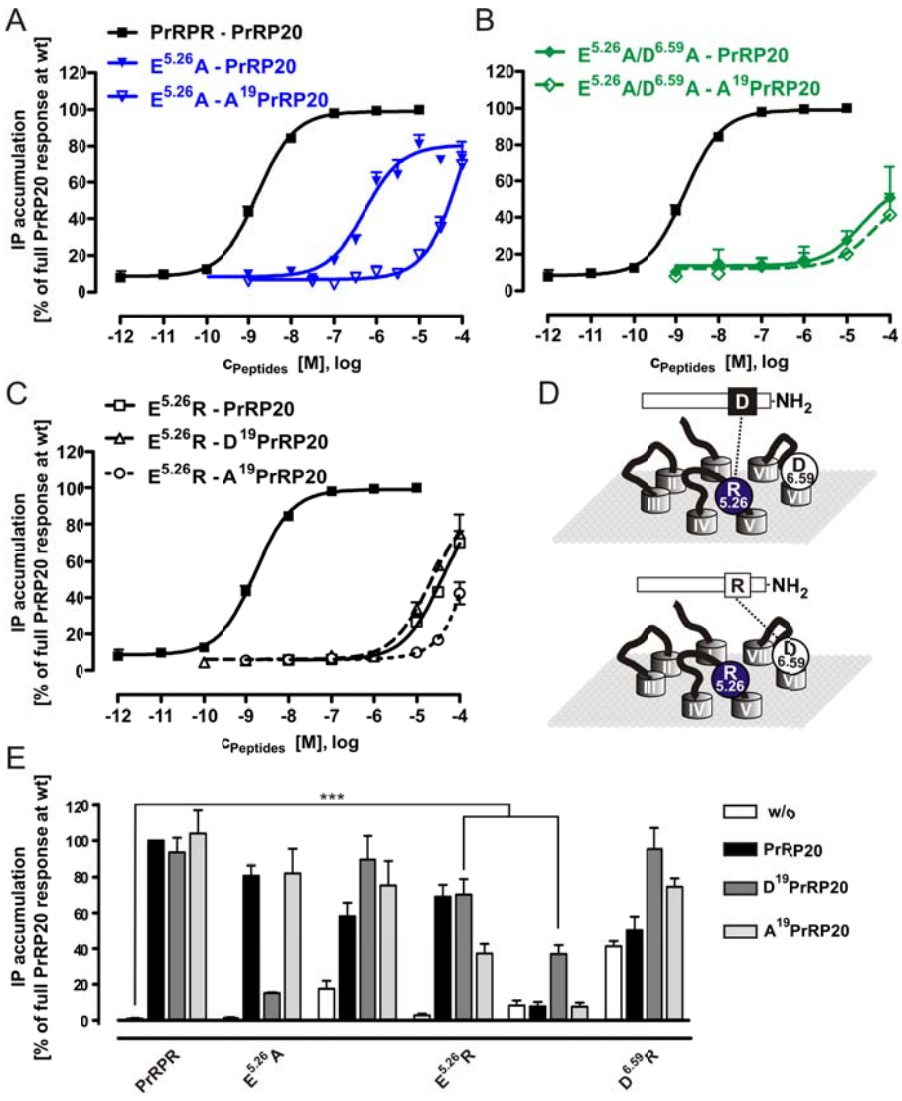

Figure 8